Mine Water and the Environment (2024) 43:449–462
https://doi.org/10.1007/s10230-024-01003-2

TECHNICAL ARTICLE

Removal of Metal(Loids) from Acid Mine Drainage Using Manganese Oxide Wastes from a Mining-Metallurgical Process

Luis F. Piñon-Flores[1] · Margarita E. Gutiérrez-Ruiz[1] · José L. González-Chávez[1] · Daniel E. Amaro-Ramírez[1] · Arturo Aguirre-Gómez[2] · Marco A. Molina-Reyes[1]

Received: 7 December 2023 / Accepted: 19 August 2024 / Published online: 13 September 2024

Abstract

This study focused on treating acid mine drainage (AMD) from a Zn-sulfide mine with a composition that includes Al = 445 mg/L, Fe = 263 mg/L, Mn = 364 mg/L, Cd = 2.8 mg/L, and Zn = 4,830 mg/L. After treatment with regional alkaline minerals, the pH increased from 3.0 to 6.3 and metal concentrations decreased mainly by precipitation, falling below Mexico's permissible limits (MPL) for river discharges, except for Cd^{2+} and Zn^{2+}, which exceeded their MPLs with concentrations of 0.4 and 1,110 mg/L, respectively. We tested the use of waste materials from a Mn mine containing Mn carbonates (R3) and Mn oxides (R6) for removal of these contaminants. Several Mn oxides have been reported as promising adsorbents and indeed the R6 waste was more efficient than the R3. At a ratio of 0.75 g/L of R6, with 30 h of contact or a ratio of 0.2 with 60 h of contact, Cd^{2+} and Zn^{2+} concentrations were decreased to below their MPLs. The evaluation of removal mechanisms was hindered by the complexity of the waste's composition. However, contact with the AMD increased the zeta potential from negative to positive values, indicating a cation sorption process. Mn wastes can be used without prior alkaline mineral treatment, but their technical and economic viability is less. The results suggest that this process is suitable for treating AMD at abandoned mines sites. Additionally, the Mn wastes can potentially be sold as a sorbent material for other processes, offering a recycling option.

Keywords AMD treatment · Mn oxides sorption capacity · AMD management · Manganese waste recycling · Sustainable mining · Soluble metal remotion

Zusammenfassung

Diese Studie konzentrierte sich auf die Behandlung von saurem Grubenwasser (AMD) aus einer Zn-Sulfid-Mine mit einer Zusammensetzung, die 445 mg/L Aluminium, 263 mg/L Eisen, 364 mg/L Mangan, 2,8 mg/L Cadmium und 4.830 mg/L Zink beinhaltet. Nach der Behandlung mit regionalen alkalischen Mineralien stieg der pH-Wert von pH 3,0 auf pH 6,3. Die Metallkonzentrationen sanken vor allem durch Ausfällungen und fielen unter die zulässigen mexikanischen Grenzwerte für Flusseinleitungen, mit Ausnahme von Cd2+ und Zn2+, die ihre Grenzwerte mit Konzentrationen von 0,4 mg/L bzw. 1.110 mg/L überschritten. Wir testeten die Verwendung von Abfallstoffen aus einer Mangan-Mine, die Mn-Karbonate (R3) und Mn-Oxide (R6) enthalten, um diese Schadstoffe zu beseitigen. Mehrere Mn-Oxide sind als vielversprechende Adsorptionsmittel bekannt, und tatsächlich war der R6-Abfall effizienter als R3. Bei einer Dosis von 0,75 g/L R6 und einer Kontaktzeit von 30 Stunden bzw. einer Dosis von 0,2 g/L und einer Kontaktzeit von 60 Stunden wurden die Cd2+- und Zn2+-Konzentrationen auf Werte unterhalb der Grenzwerte gesenkt. Die Bewertung der Entfernungsmechanismen wurde durch die Komplexität der Abfallzusammensetzung erschwert. Der Kontakt mit dem sauren Grubenwasser führte jedoch zu einem Anstieg des Zetapotenzials von negativen zu positiven Werten, was auf einen Kationensorptionsprozess hindeutet. Mn-Abfälle können ohne vorherige Behandlung mit alkalischen Mineralien verwendet werden, aber ihre technische und wirtschaftliche Rentabilität ist geringer. Die Ergebnisse deuten darauf hin, dass dieses Verfahren für die Behandlung von AMD in stillgelegten Bergwerken geeignet ist. Darüber hinaus können die Mn-Abfälle potenziell als Sorptionsmittel für andere Verfahren verkauft werden, was eine Recyclingoption darstellt.

Extended author information available on the last page of the article

Introduction

Current management of acid mine drainage (AMD) primarily involves the implementation of either active or passive treatment, which can be biotic or abiotic. Active treatment, a key component of AMD management, involves the strategic use of chemicals to raise pH levels, thereby facilitating the precipitation of metal(oid) ions. While active systems require continuous chemical dosing, power consumption, and regular operation and maintenance, their reliability is a major advantage (RoyChowdhury et al. 2015). These methods can be engineered to accommodate any pH, flow rate, or acidity load and are not limited by tight operational parameters like passive systems can be (Taylor et al. 2005). Active treatment plants using limestone, hydrated lime, pebble quicklime, soda ash, caustic soda, ammonia, or steel slag, are mainly found at operating or recently operating mines.

In contrast, passive treatment systems are typically used at closed and abandoned mines (Trumm 2010), because the systems' operation and maintenance requirements are relatively low (Berghorn and Hunzeker 2001; Yang et al. 2023). Additionally, passive techniques are environmentally friendly as they conserve energy and can provide habitat for plants and wildlife (Ford 2003; Hengen et al. 2014; Martínez et al. 2019). However, these treatments generally have longer remediation times than active processes and require periodic inspection and maintenance (Ford 2003). In any case, for active or passive treatments, it's essential to consider that long-term monitoring is necessary until AMD generation stops, due to the persistent nature of sulfur oxidation, which can last for centuries (Park et al. 2019).

Therefore, it is necessary to carefully select an appropriate AMD treatment method, whether active or passive, to achieve a successful process. Funding and operational logistics influence this decision (Cravottta III 2021), and other factors must also be considered, such as waste characteristics, pH, flow rate, construction area size, local topography, and environment (RoyChowdhury et al. 2015). Trumm (2010) proposed an analytical framework for decision-making on the feasibility of using either a passive or active treatment method at a specific site, mainly based on these factors. His strategy was based on the method's technical effectiveness and cost.

In Taxco Guerrero, a hybrid passive treatment system (abiotic + biotic) was developed to control AMD at historic and abandoned sites and tested at a non-operational zinc (Zn) mine. The selection of a passive tailor-made treatment for the study site was based on an analysis of the technical and scientific factors as reported by Trumm (2010): (a) the mine is inactive; (b) there is a large area for construction; (c) the drainage pH > 2; the flow is discontinuous because the acid drainage is mainly formed in the rainy season (≈ 420 to 3,104 L/min) (Ramos-Perez et al. 2022); and (d) the treatment uses local materials and wastes from a nearby Mn mining-metallurgic complex, and does not consume electricity.

The AMD is generated in underground tunnels in the Zn mine. According to Romero et al. (2011), the acidic effluent (pH 2.2–2.9) contains high concentrations of the following ions in mg/L: sulfates (1,470–5,454), Zn (3.0–859), Fe (5.5–504), Cu (0.7–16.3), Cd (0.3–6.7), Pb (0.05–1.8), and As (0.002–0.6); with an oxidation-reduction potential (ORP) ranging from 690 to 710 mV (Pérez-Corrales 2015). The treatment design consists of 10 sequentially installed open ponds on the ground (Pérez-Corrales 2015; Ramos-Perez et al. 2022; Romero et al. 2011). The first eight ponds are used to homogenize the AMD and combine it with local calcareous shales and other materials to counteract the acidity, settle solids, and filter the AMD (see supplemental Fig. S-1). Subsequently, the remaining two ponds form a wetland; the final effluent of the abiotic process is biologically treated as outlined by Ramos-Perez et al. (2022). This process reduces the concentrations of most metal(oid) ions to levels compliant with Mexico's environmental regulations (NOM-001-SEMARNAT-2021) for river discharge. However, Cd^{2+} and Zn^{2+} concentrations remained elevated, with final concentrations exceeding the maximum permissible limits (MPLs) of 0.2 for Cd^{2+} and 10 mg/L for Zn^{2+}; the minimum values reached were 1.02 and 349 mg/L, respectively (Ramos-Perez et al. 2022). In AMD with high ionic strength, the pH needed to precipitate those metals as insoluble hydroxides (Pérez-Corrales 2015) is higher than is achievable with regional alkaline minerals. Hydrated lime or other alkaline materials could be used to increase the pH to over 8.5 but would greatly increase the treatment costs. So, instead, we investigated potential sorbing agents that were available, Mn oxides and Mn carbonates. Several studies have reported their effectiveness as sorbents and scavengers of contaminants (Islam et al. 2018; McKenzie 1972; Wang et al. 2020; Xiong et al. 2017; Zhang et al. 2020). They possess a high specific surface area (SSA), surface charge, polymorphic nature, and natural availability. Some studies have reported high cation and anion sorption capacities of manganese carbonates, such as fluoride, Cu, Cd, Pb, and Zn (Della et al. 2013; Demirkiran 2015; Zhang and Jia 2018). Indeed, using these wastes to treat AMD can be effective and environmentally friendly (Feng et al. 2007; Islam et al. 2018).

Mining wastes with high concentrations of Mn-oxides and Mn-carbonates are available in a Mn mine-metallurgical unit located in the province of Molango, Hidalgo, Mexico (400 km from Taxco), which is one of the world's most notable global deposits of Mn (Molina & Piñon 2019). MnO nodules are produced in a rotary furnace there. Two waste materials were sampled: R3, which is 31% Mn, is a residual

$MnCO_3$ dust collected from before the ore enters the rotary furnace, and R6, which are particles < 0.64 cm (< ¼ in) in diameter with a slightly higher Mn content (33.5% MnO) from the final stage of the rotary furnace. Both materials are rejected from the metallurgical process because their particle size is too small to produce MnO nodules, the unit's main product. The objective of the research was to evaluate the efficacy of utilizing these two Mn wastes, which are rich in carbonates and/or oxides, in mitigating the concentrations of Zn^{2+} and Cd^{2+} in the AMD. This paper reports the results of laboratory tests conducted to assess the potential effectiveness of these Mn wastes, with or without adding local alkaline minerals, on the removal of Zn^{2+} and Cd^{2+} to facilitate the remediation of AMD at historical non-active mines, while also improving the recycling of mining wastes. The objective of this treatment process was to demonstrate a circular economy solution that will protect the environment and transform our current culture of waste disposal into one of waste valorization.

Methodology

Sampling and Preparation

In the Taxco mining area, samples of AMD were collected from each of the ten serial passive treatment ponds (P0 to P9) (supplemental Figure S-1). Two liters from each pond were transferred into high-density Nalgene bottles (500 mL each) with airtight lids, stored at 4 °C, and transported to the laboratory for analysis and experiments. Furthermore, 10 samples ≈ 1 kg each were collected from the two waste products resulting from the MnO nodulization processes at the mining-metallurgical complex. These samples were combined to create two composite solid waste samples. The samples were collected using steel scoops, transferred into hermetically sealed plastic bags, and transported to the laboratory. They were dried at 45 °C for 48 h, ground, sieved to pass through a #100 (0.149 mm) mesh, and homogenized by quartering (Hesse 1971). Aliquots of 100 g were prepared and combined to create 1 kg of composite samples for each waste. Aliquots (100 g) for chemical analysis were milled, sieved (#200 mesh < 0.074 mm), and dried at 96 °C. The samples were stored in airtight containers at room temperature (15–20 °C) until analysis.

Analytical Determinations

The analyses were conducted by the LABQA laboratory (accredited by the "Accreditation Body in Mexico") at the School of Chemistry, National Autonomous University of Mexico (UNAM). A QA/QC analytical procedure was followed for sampling and analytical reproducibility, which included preparing blanks and duplicates using spiked samples and certified international reference material (high purity standards QCS-26-100 for ICP-OES analysis), ultrapure deionized water, and analytical-grade or high-purity reagents.

The pH was measured using the U.S. EPA-9045D method (EPA 2004) with a Thermo-720 potentiometer at 25 °C. Electrical conductivity (EC) was determined in accordance with the EPA-120.1 method (EPA 1982) using Corning-441 equipment.

The AMD samples were digested by mixing 7 mL with 3 mL of concentrated nitric acid and heating them in an Ethos Easy Milestone microwave, following the U.S. EPA-3015 A method (EPA 2007). Mineral solid samples were digested following the general conditions described in the U.S. EPA-3052 method (EPA 1996). Portions of 0.2 (± 0.0001) g of each solid sample were placed in an open digestion system using 3 mL of concentrated nitric acid, 2 mL of concentrated hydrochloric acid, and 5 mL of concentrated hydrofluoric acid (analytical grade). The mixture was heated to 120 °C to complete the digestion and then filtered using Whatman no. 42 filter paper (2.5 mm). The resulting samples were stored in airtight Nalgene bottles at 4 °C.

The Al, Mn, As, Fe, Cd, and Zn, were quantified using inductively coupled plasma-optical emission spectrometry (ICP-OES) equipment (Agilent Technologies AG-5100) following the U.S. EPA-6010 C method (EPA 2000). Additionally, the elemental composition of the solid Mn waste samples was determined using a portable x-ray fluorescence (PXRF) analyzer (Olympus model DP-6000, Olympus Scientific Solutions, MA, USA), according to the U.S. EPA method 6200 (EPA 2007b). For quality control purposes, the National Institute of Standards and Technology (NIST) SRM 2710a "Highly Elevated Trace Element Concentrations" and SRM 2711a "Moderately Elevated Trace Element Concentrations" were used. The quality control parameters are presented in supplemental Table S-2. The average recoveries of the elements of interest were 90–110%, and the coefficients of variations were < 10%. The use of portable XRF for analyzing metal concentration in solid samples has been widely documented (Bower et al. 2017; Meza-Figueroa et al. 2020; Turner and Lewis 2018). All the analyses were conducted in triplicate and the results were then averaged.

The SEM-EDS analyses were performed using a Hitachi TM1000 tabletop scanning electron microscope with an energy-dispersive spectroscopy module. The geochemical crystalline compositions of the solid samples were determined by XRD using an Empyrean instrument equipped with a Ni-filter, fine-focus copper tube, and PIXcel3D detector. The measurements were conducted in the angular interval 2θ from 4° to 80° using a "step scan" of 0.003° (2

Theta) and an integration time of 40 s per step. Quantification was performed using the Rietveld method, which was implemented in the HIGH Score v4.5 software and utilizing the ICDD (International Center for Diffraction DATA) and ICSD (Inorganic Crystal Structure Database).

The zeta potential (ZP) was measured using the Zeta-Meter 3.0 + equipment within a pH range of 3 to 9 at various concentrations of $ZnSO_4 \cdot H_2O$.

Preliminary Experiment

A preliminary factorial experiment was conducted to approximate the Mn-wastes' capacity for removing metal(oids) from AMD. The samples of the treated acid solution from the passive treatment that were tested were from the initial (P0), intermediate (P5), and final (P9) ponds. The R3 sample was selected and tested due to its high carbonate content, which facilitates rapid AMD neutralization and removal through sorption and/or precipitation. The R3 waste was mixed with the three AMD samples (P0, P5, and P9) at three solid/liquid (s/l) ratios (1.5, 2.5, and 3 g/25 mL). Three solid-liquid contact times were proposed: 20 and 60 min with axial agitation and 18 h without stirring. Duplicates were conducted for 27 trials and the pH and identified metal(oids) in the AMD were monitored (Al, As, Cd, Fe, Mn, Pb, Zn). The factorial experiment conditions are presented in supplemental Table S-3.

Experiment Designed by Minitab

Experiments were designed using the Minitab statistical software to establish the best conditions for reducing the Zn^{2+} and Cd^{2+} concentrations in AMD below their MPLs. This tool generates a comprehensive design encompassing all considered variables while greatly reducing the required trials. Typically, the central composite design provided by Minitab is employed after conducting a factorial or fractional factorial experiment and identifying the most critical factors in the process. Once the design is created, Minitab stores the design information in the worksheet, specifying the order for data collection. Following data collection, the analysis is performed using its Analyze Response Surface Design feature. The design of experiments in Minitab permits the implementation of a sequential experimentation approach, whereby a set of smaller experiments are conducted, with the results at each stage guiding the experimentation at the subsequent stage. The sequential approach has the advantage that only a limited number of experimental trials are conducted at each stage, reducing the likelihood of resources being expended on unproductive trials. However, it is recommended that the results of a specific experiment be checked before applying the optimal combination at the pilot scale.

In this instance, the software was supplied with an extreme contact time range (120 h and 24 h) and ratios of waste/AMD (2 g/15 mL and 0.5 g/15 mL) from the preliminary experiment. Based on this data, the software generated the following contact times: T1 = 4.12 h, T2 = 24 h, T3 = 72 h, T4 = 120 h, and T5 = 139.8 h for R3 and R6 wastes and AMD from the P9 pond. The ratios for five concentrations (C1 to C5) were 0.189 g/15 mL, 0.5 g/15 mL, 1.25 g/15 mL, 2 g/15 mL, and 2.31 g/15 mL. The solid-to-liquid ratios and contact time were adjusted for each waste and AMD sample, as outlined in supplemental Table S-4. The software assessed the influence of each variable and their combined effects. Scenarios, depicted as curves, were constructed by extrapolating experimental data with 95% confidence (Fig. 1).

Zeta Potential

The ZP of the R3 and R6 wastes was determined at different pH values. The ZP is an important indicator of the superficial charge of colloids and explains ionic retention. Positive sites favor anion retention and negative charges favor cationic retention. The ZP is measured by adding a solution to a cell containing two gold electrodes. When a voltage is applied to the electrode, particles move toward the electrode with the opposite charge. The Doppler technique is used to measure the particles' velocity as a voltage function.

- **First test**. One gram of each waste was mixed with 500 mL of deionized water. Eight aliquots were prepared from each stock solution, and the pH was adjusted to different values between 3 and 10 with HCl and NaOH. Solutions were shaken until equilibrium was attained (pH constant). The ZP was measured, and several determinations' average value (mV) was reported.
- **Second test**. The ZP of the R3 and R6 samples in contact with AMD from the P9 pond at a pH of ≈ 7 were measured at different concentrations and times: (a) C2T4, (b) C3T1, (c) C3T5, and (d) C4T2 (Table S-4).
- **Third test**. The ZP of the R3 and R6 wastes was determined at different Zn^{2+} concentrations at circumneutral pH values under the following conditions: (a) original Zn^{2+} concentration in AMD, (b) AMD + 1,000 mg Zn^{2+}/L, (c) AMD + 2,000 mg Zn^{2+}/L, and (d) AMD + 5,000 mg Zn^{2+}/L. The suspensions were filtered using syringes with membranes with a pore size of 0.05 µm, and the solutions were acid digested. The Zn^{2+} concentrations were quantified by ICP-OES following the EPA-6010 C method (EPA 2000).

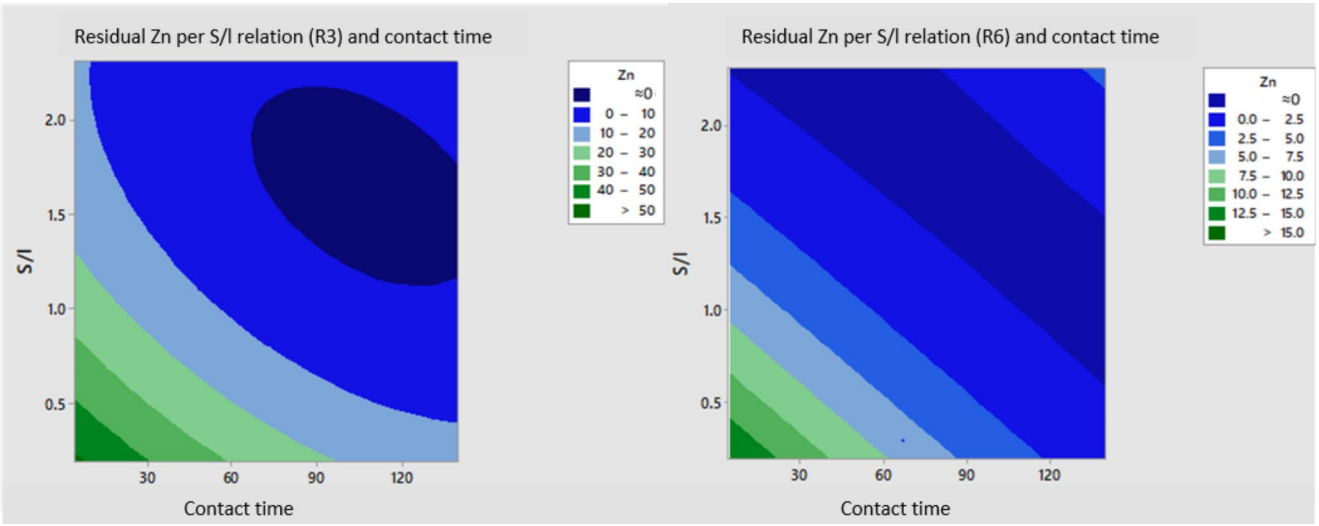

Fig. 1 Contour plot of Mn wastes (R3 and R6)/ AMD-P9 ratios vs. contact time (hours) indicating final concentration of Zn2 + in treated AMD based on the extrapolation of Minitab software

Sequential Extraction

The method for sequential extraction was modified from Tessier et al. (1979).

Fraction (I): Exchangeable. The sediment underwent extraction at room temperature for 1 h using 8 mL of either magnesium chloride solution (1 M $MgCl_2$, pH 7.0) or sodium acetate solution (1 M NaOAc, adjusted to pH 8.2) with continuous agitation.

Fraction (II): Bound to Carbonates: The residue from Fraction (I) was leached at room temperature with 8 mL of 1 M NaOAc adjusted to pH 5.0 with acetic acid (HOAc). Continuous agitation was maintained, and the duration required for complete extraction was assessed.

Fraction (III): Bound to Fe-oxides: The residue from Fraction (II) underwent extraction with 20 mL of 0.3 M $Na_2S_2O_4$ + 0.175 M Na-citrate + 0.025 M H-citrate. These experiments were conducted at 96 ± 3 °C with occasional agitation and the time for complete dissolution of the free iron oxides was recorded.

Fraction (IV): Residual: The residue from Fraction (III) was digested with HF-$HClO_4$ (5:1).

Results and Discussion

Characterization of AMD

Table 1 displays the pH, EC, and total elemental concentrations of Al, As, Cd, Fe, Mn, Pb, and Zn in AMD. The pH of the AMD increased markedly with the addition of local alkaline materials throughout the successive steps of the passive treatment. The pH ranged from 3.0 in the P0 pond (non-treated AMD) to 4.8 in the intermediate pond (P5) and reached 6.3 in the final treatment (P9) (Table 1). The decrease in EC was insignificant, with a change from 3.0 to 2.4, suggesting the presence of soluble ions throughout the entire treatment.

Table 1 displays the primary components of the AMD were Al, Fe, Zn, and Mn, and their concentrations decreased as the pH increased. The elements with greater removal rates were Al (reduced from 445 to < 0.2 mg/L) and Fe (reduced from 263 to < 0.1 mg/L). Starting from the P7 pond, the concentrations of these two elements fell below their detection limits (LODs) (Table 1). After reaching P9 in the final stage of the alkaline treatment, the Zn concentration dropped from 4,830 to 1,110 mg/L, representing a marked reduction but as mentioned earlier, still exceeding the MPL for treated water discharged into rivers (Zn = 10 mg/L, monthly average). The Cd^{2+} concentration changed from 2.8 mg/L in the P0 pond to 2.5 mg/L in P5 and 0.4 mg/L in P9, representing a notable decrease, but still exceeding its MPL (0.2 mg/L, monthly average) (Table 2).

The concentrations of Pb and As were below the LODs (0.02 and 0.1 mg/L) and the MPL in the AMD from P9 (non-treated) (Table 1). The concentrations of Al and Fe in the AMD at the initial step of the passive treatment were less than expected, but Al and Fe ions can form solid oxi-hydroxides and hydroxy sulfates, such as jarosite or goethite-bearing Fe (III), under acidic conditions (Ryu and Kim 2022; Webster et al. 1998). These compounds can retain Pb and As, thereby lowering their concentrations in non-treated AMD. However, it's also possible that the Pb could have partially precipitated as $PbSO_4$ (Kumpiene 2010).

The soluble sulfate concentration in AMD ranged from 1,700 (P9) to 12,249 mg/L on P0 (not presented). The

Table 1 pH, EC, and Elemental Total Concentration of metal(oids) in AMD

Code	Concentration of the elements (ICP-OES)								
	pH	C.E. (mS/cm)	Al (mg/L)	As (mg/L)	Fe (mg/L)	Mn (mg/L)	Cd (mg/L)	Zn (mg/L)	Pb (mg/L)
LOD (mg/L)			0.2	0.1	0.1	0.2	0.1	0.1	0.02
Permissible Level (MPL for Rivers, mg/L) (NOM-001-SEMARNAT-2021)									
Monthly Average	6a-9	non controlled	non controlled	0.2	non controlled	non controlled	0.2	10	0.2
Daily Average				0.3			0.3	15	0.3
Instant Value				0.4			0.4	20	0.4
P0	2.9(±) 0.5	3.0	445(±) 31	< LOD	263(±) 17	364(±) 36	2.8(±) 0.2	4,830(±) 322	< LOD
P1	2.8(±) 0.5	3.4	534(±) 38	< LOD	277(±) 18	417(±) 41	2.9(±) 0.2	5,250(±) 350	< LOD
P2	4.4(±) 0.5	3.0	133(±) 9.3	< LOD	0.2(±) 0.01	401(±) 40	2.7(±) 0.2	4,650(±) 310	< LOD
P3	4.2(±) 0.5	2.8	210(±) 15	< LOD	0.4(±) 0.02	380(±) 37	2.7(±) 0.2	4,710(±) 314	< LOD
P4	4.9(±) 0.5	2.8	0.3(±) 0.02	< LOD	< LOD	337(±) 33	2.5 (±)0.2	3,640(±) 242	< LOD
P5	4.8(±) 0.5	2.7	4.6(±) 0.3	< LOD	0.2(±) 0.01	347(±) 34	2.5(±)0.2	3,600(±) 240	< LOD
P6	5.2(±) 0.5	2.5	0.2(±) 0.02	< LOD	< LOD	324(±)32	2.3(±) 0.2	5,680(±) 379	< LOD
P7	5.3(±) 0.5	2.4	< LOD	< LOD	< LOD	312(±) 31	2.1(±) 0.2	2,970(±) 198	< LOD
P8	5.8(±) 0.5	2.4	< LOD	< LOD	< LOD	311(±) 30	1.4(±) 0.1	2,310(±) 154	< LOD
P9	6.3(±) 0.5	2.4	< LOD	< LOD	< LOD	279(±) 27	0.4(±) 0.03	1,110 (±) 74	< LOD

Table 2 Cd^{2+} and Zn^{2+} concentrations (mg/L) determined by ICP-OES in the ADM of fifty-four tests from the experiment designed by Minitab software

Code	Cd	Zn	Code	Cd	Zn
Detection limits	0.01	0.01	Detection limits	0.01	0.01
P0-R3-C1T3	2.2 ± 0.04	318 ± 3	P0-R6-C1T3	1.8 ± 0.1	241 ± 12
P0-R3-C2T2	1.7 ± 0.01	300 ± 7	P0-R6-C2T2	1.5 ± 0.2	214 ± 10
P0-R3-C2T4	1.3 ± 0.01	244 ± 4	P0-R6-C2T4	0.8 ± 0.2	117 ± 7
P0-R3-C3T1	1.3 ± 0.01	275 ± 5	P0-R6-C3T1	1.3 ± 0.1	182 ± 7
P0-R3-C3T3	0.8 ± 0.3	212 ± 13	P0-R6-C3T3	0.3 ± 0.3	33 ± 4
P0-R3-C3T5	0.6 ± 0.02	175 ± 17	P0-R6-C3T5	0.2 ± 0.1	10 ± 1
P0-R3-C4T2	0.7 ± 0.4	208 ± 21	P0-R6-C4T2	0.5 ± 0.1	55 ± 8
P0-R3-C4T4	0.3 ± 0.01	137 ± 2	P0-R6-C4T4	0.03 ± 0.02	2.0 ± 0.2
P0-R3-C5T3	0.4 ± 0.1	127 ± 5	P0-R6-C5T3	0.1 ± 0.01	6.3 ± 0.6
P5-R3-C1T3	1.2 ± 0.01	204 ± 6	P5-R6-C1T3	1.4 ± 0.1	179 ± 19
P5-R3-C2T2	0.7 ± 0.01	183 ± 1	P5-R6-C2T2	1 ± 0.2	146 ± 8
P5-R3-C2T4	0.7 ± 0.1	166 ± 1	P5-R6-C2T4	< LOD	0.4 ± 0.1
P5-R3-C3T1	0.7 ± 0.01	182 ± 1	P5-R6-C3T1	0.8 ± 0.1	138 ± 14
P5-R3-C3T3	0.3 ± 0.1	120 ± 13	P5-R6-C3T3	0.1 ± 0.04	13 ± 2
P5-R3-C3T5	0.3 ± 0.1	108 ± 7	P5-R6-C3T5	0.02 ± 0.01	0.7 ± 0.5
P5-R3-C4T2	0.2 ± 0.02	111 ± 12	P5-R6-C4T2	0.1 ± 0.01	17 ± 2
P5-R3-C4T4	0.2 ± 0.01	82 ± 11	P5-R6-C4T4	< LOD	0.4 ± 0.1
P5-R3-C5T3	0.1 ± 0.01	72 ± 8	P5-R6-C5T3	< LOD	0.8 ± 0.2
P9-R3-C1T3	< LOD	34 ± 2	P9-R6-C1T3	< LOD	5.2 ± 0.5
P9-R3-C2T2	< LOD	24 ± 2	P9-R6-C2T2	< LOD	10.7 ± 0.7
P9-R3-C2T4	< LOD	4.1 ± 0.3	P9-R6-C2T4	< LOD	1.4 ± 0.1
P9-R3-C3T1	< LOD	28 ± 2	P9-R6-C3T1	< LOD	3.7 ± 0.2
P9-R3-C3T3	< LOD	2.9 ± 0.2	P9-R6-C3T3	< LOD	0.6 ± 0.04
P9-R3-C3T5	< LOD	0.9 ± 0.1	P9-R6-C3T5	< LOD	< LOD
P9-R3-C4T2	< LOD	4.16 ± 0.28	P9-R6-C4T2	< LOD	0.8 ± 0.1
P9-R3-C4T4	< LOD	0.63 ± 0.04	P9-R6-C4T4	< LOD	< LOD
P9-R3-C5T3	< LOD	1.15 ± 0.08	P9-R6-C5T3	< LOD	< LOD

sulfate ions coordinate the Zn^{2+} and Cd^{2+} forming complexes, preventing their partial or total precipitation at the pH reached. The decrease in Mn concentration in the AMD during the neutralization process is relatively low (Table 1). However, the maximum permitted level in water bodies is not regulated in Mexico.

Characterization of Mining-metallurgical Wastes

R3 is mainly formed by dust from a collector located before the thermic process, where the carbonates are decomposed to form Mn oxides. Therefore, its composition must be like the original mineral that feeds the process, with an elevated concentration of $MnCO_3$. This explains the strong reaction of R3 with HCl (supplemental Table S-5). Conversely, R6 is a waste from the furnace, only rejected because its size is less than required. Therefore, as the final product, it has a high content of Mn-oxides formed by the thermal decomposition of $MnCO_3$ but also contains some of this mineral, possibly because some R3 wastes are occasionally stored in the open-air disposal site. Both Mn wastes are basic; R3 has a pH of 10.5 and R6 of 8.6, according to the CO_3^{2-} content, explaining its different reaction with HCl (Table S-5). The EC of R3 is less (263 mS/cm) than the EC of R6 (7,810 mS/cm) (Table S-5) because the oxidation of traces of pyrite from the Mn-ore in the furnace forms some soluble salts.

The pseudo-total concentrations ($HNO_3 + H_2O_2$) of metals in both wastes are: Mn in R3=(27.9–34.1%) and R6=(30.2–36.8%), Fe in R3 =(3.7%-4.2) and R6=(5.4–6.1%), Al in R3 (0.3–0.3%) and R6=(0.2–0.2%), Zn in R3 = (83–95 mg/kg) and R6=(190–217 mg/kg) (supplemental Table S-6). The total concentrations by XRF are: Mn in R3= (35.4–43.3%) and R6= (38.3–46.9%), Fe in R3= (11 -13.5%) and R6= (11.5–14%), Al in R3= (7.6–9.4%) and R6= (4.8–5.9%). The higher relative Mn concentration in R6 than in R3 results from the matter loss related to the formation of CO_2 and SO_2 during the heating treatment. The similar composition between R6 and the final product of the metallurgic process (nodules) results from the fact that R6 is rejected from the nodulization process only because of its particle size.

Table 3 Minerology of R3 and R6

Minerals		% Relative in crystalline phase	
		R3	R6
Rhodochrosite	$MnCO_3$	34.6	27.4
Galaxite	$Mn^{2+}Al_2O_4$	-	20.2
Ribbeite	$Mn^{2+}{}_5(SiO_4)_2(OH)_2$	-	19.3
Gypsum	$CaSO_4\ 2H_2O$	-	9.9
Hausmannite	$Mn^{2+}Mn^{3+}{}_2O_4$	-	8.5
Quartz	SiO_2	12.4	6.3
Magnetite	Fe_3O_4	5.2	1.8
Manganosite	MnO	-	1.7
Clinopiroxene	$(Ca, Mg, Fe)_2(Si, Al)_2O_6$	-	1.3
Tephroite	$(Mn^{2+})_2SiO_4$	-	1.2
Todorokite	$(Na, Ca, K, Ba, Sr)1\text{-}x\ (Mn, Mg, Al)_6O_{12} \cdot 3\text{-}4H_2O$	-	1
Calcium Magnesium Iron Carbonate Dolomite	$Ca\ (Mg, Fe)\ (CO_3)_2$	20.5	-
Sodium Zinc Phosphate Hydrate	$Zn_2\ Na\ P_3\ O_{10}\ 9H_{20}$	20.3	-
Pyrite	FeS_2	7	-

The soluble concentrations of the Zn, Cd, Pb, As, Se, Cu, and Fe in R3 and R6 recovered with meteoric water (deionized water in equilibrium with CO_2, pH = 5.5) are less than the LOD of ICP-OES (data not presented), suggesting that their compounds have very low solubility under environmental conditions. Based on these results, it is assumed that R3 and R6 are not important sources of soluble toxic metals. The sequential extraction of Mn indicates that this element is recovered in the following fractions: residual (R3 = 83%, R6 = 76%), oxides, and carbonates (R3 = 10%, R6 = 15%), with the rest distributed in other fractions. The soluble Mn concentration in meteoric water in R3 is 29 mg/L and in R6 is lower than the LOD (0.2 mg/L).

To identify the main minerals of the wastes, three diffractograms of each waste were obtained. Supplemental Figs. S-2 and S-3 present examples of one diffractogram for each waste, and their relative percentages in the crystalline phase are reported in Table 3. In the six diffractograms obtained, some similarities are observed. Rhodochrosite was identified in R3 and R6, but in R3, it was the dominant mineral with a relative percentage between 34.6 and 60.9, and in R6, it was between 15.3 and 27.4%. In R3, no Mn oxides were identified, while in R6, Mn oxides II, III, and IV were found in variable percentages from 1.7 to 20.2%, with more Mn II and III oxides (galaxite ($Mn^{2+}Al_2O_4$), manganite [$Mn^{3+}O(OH)$], hausmannite [$(Mn^{2+}, Mn^{3+})_2O_4$], pyrolusite (MnO_2), manganosite (MnO), magnetite Fe_3O_4, and todorokite (Na, Ca, K, Ba, Sr) 1-x (Mn, Mg, Al)$_6O_{12}$ 3–4 H_2O) than Mn IV oxides. Some of the Mn minerals identified in R6 were found in the final product (pellets) (personal communication-mining company). They are manganosite, tephroite (Mn_2SiO_4), and galaxite [(Mn, Mg) Al_2O_4.]. The XRD diffractogram of sample R3 indicates the dominant presence of rhodochrosite as mentioned above and minor concentrations of Ca/Mg/Fe carbonates, quartz, pyrite, and magnetite (Table 3, supplemental Figs. S-2 and S-3).

The amorphous background partially covered the XRD signals, mainly of minerals in low concentrations in R3 and R6, like those of Zn^{2+} and Cd^{2+}. The crystalline materials are scarce in wastes from thermic processes or Mn ores, where amorphous material is abundant. The amorphous Mn

oxides have been reported as substances with higher sorption capacity than their crystalline counterparts (Al-Degs et al. 2001; Dyer et al. 2000; Islam et al. 2018; Wick et al. 2019; Zhang et al. 2016), which is convenient to this case. The diversity in amorphous content and mineral composition is a crucial aspect to consider as it could explain the different sorption behaviors of R3 and R6. It is important to note that R6 is the only waste with Mn oxides with high sorbent capacity (Xiong et al. 2017; Zhang et al. 2020).

The results of the SEM-EDS particle analysis of R3 and R6 (Fig. 2) were consistent with the elemental composition of the entire sample determined by ICP and XRF (supplemental Tables S-6 and S-7). The elements identified in the 10 particles analyzed by SEM-EDS are Mn, Fe, and Ca, and Si, Al, Mg, and S were found in some particles. Comparing the media of those elements in all particles, the Mn concentration is greater in the R6 particles, similarly to the total analysis values, due to the loss of CO_2 that reduced the total mass. In the rest of the elements, the concentrations in the analyzed particles were similar for Fe, Al, and Mg or less, as in the case of S, due to SO_2 losses in the furnace.

Preliminary Experiment

The addition of R3 to AMD from pond P0 (non-treated) at different solid/liquid ratios (C1, C2, C3) increased the pH even with the smallest amount of contact time and quantity of waste added. The pH changed to near-neutral values in

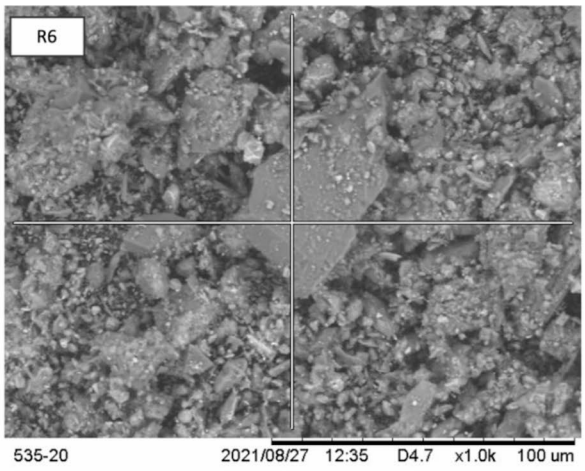

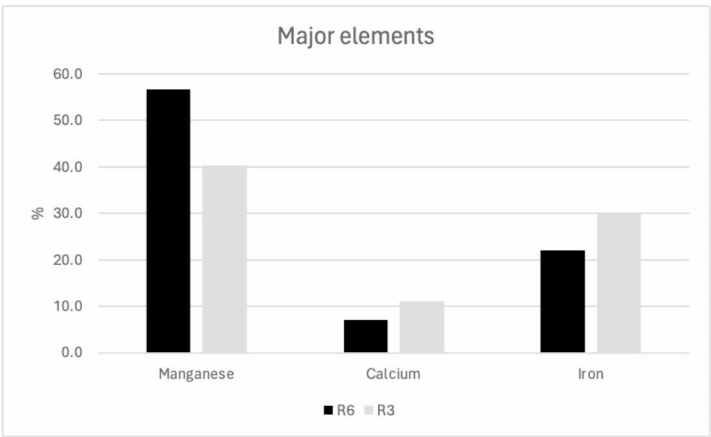

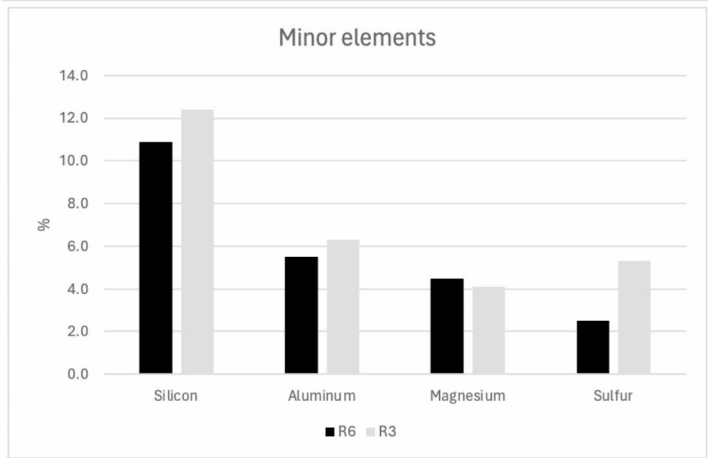

SAMPLE		(Data from ten particles subjected to analysis)						
		Mn	Fe	Si	Ca	Al	Mg	S
R6	Mean	56.7%	22.0%	10.9%	7.1%	5.5%	4.5%	2.5%
	Min	37.9%	15.6%	3.9%	3.5%	3.4%	3.5%	2.3%
	Max	100.0%	29.5%	22.4%	13.0%	7.0%	5.1%	2.6%
	Desvest	17.5%	5.1%	6.0%	3.1%	1.2%	0.6%	0.2%
R3	Mean	40.3%	30.0%	12.4%	11.0%	6.3%	4.1%	5.3%
	Min	25.9%	22.0%	4.1%	6.3%	5.0%	2.9%	3.3%
	Max	56.5%	40.3%	27.9%	20.8%	8.8%	5.7%	8.1%
	Desvest	9.4%	7.3%	7.2%	4.4%	1.4%	1.2%	2.5%

Fig. 2 SEM-EDS of selected particles from R3 and R6

the pond P0 AMD, shifting from 2.9 ± 0.5 to 6.4–6.6, in P5 from 4.8 to 6.5–6.8, and in P9 from 6.3 to 6.7-7.0 (supplemental Table S-8). All trials shown in Table S-8 indicate a marked removal of soluble elements, primarily Al (P0: 93–95%, P5: 93–98%, P9: 96–99%) and Fe (P0: 93–95%, P5: 93–98%, P9: 96–99%). However, reducing acidity does not sufficiently eliminate Cd and Zn to meet regulatory standards (Balintova and Petrilakova 2011). The Zn^{2+} removal in P0 was: 93–95% and in P5: 95–98%, while Cd^{2+} removal in P0 was: 14–80% and in P5: 91%. In pond P9, the final AMD pre-treatment step, the addition of R3 increased the removal efficiency. The Cd^{2+} concentration dropped below the MPL (0.2 mg/L), but not the Zn^{2+} concentration. When R3 was added at the highest concentration (3 g/25 mL), both Cd^{2+} and Zn^{2+} concentrations decreased to MPL or lower values, regardless of the contact times.

Comparison of the preliminary experiment results with the AMD from ponds P0 to P9 indicates that pretreatment with alkaline materials yields favorable results (Table S-8). Adding R3 or R6 wastes to AMD from pond P9 reduces the need for acid neutralization, thereby enhancing the sorption capacity of both P5 and P9.

Experiment Designed Using Minitab Software

The addition of the two Mn wastes to the three selected ponds (P0, P5, and P9) was effective in PTE removal. In all trials, the elements Al, As, Cu, Cr, Fe, Ni, and Pb were < 1 mg/L, and the Cd^{2+} ranged from < LOD to 2.2 mg/L and the Zn^{2+} concentrations from < LOD to 241 mg/L (Table 2).

The removal efficiencies of R3 and R6 were improved when the wastes were added to the pre-treated mine water (P9 with pH = 6.3). When R3 was used to treat the AMD from P0 and P5, the Zn^{2+} concentrations exceeded their MPLs (Fig. 3), but in 11% of the trials, the Cd^{2+} was below the MPL. With R6 used to treat AMD from P0, P5, and P9, only in 72% of the trials did the final Zn^{2+} and Cd^{2+} concentrations drop below their MPLs. However, with more prolonged contact times, R6 with AMD from P0 (non-treated AMD) at higher solid/solution ratios (C4T4 and C5T3) could reduce the final concentrations of Zn^{2} + and Cd^{2+} to levels below the MPLs. In summary, the final Zn^{2+} and Cd^{2+} concentrations were less than their MPLs in 66.6% of all the trials using R3 to treat P9 and 88.8% using R6 (Fig. 3). The dissolved Mn concentration was only slightly increased by all the R3 and R6 wastes treatments (Table S-8) and is an element for which discharge into rivers is permitted.

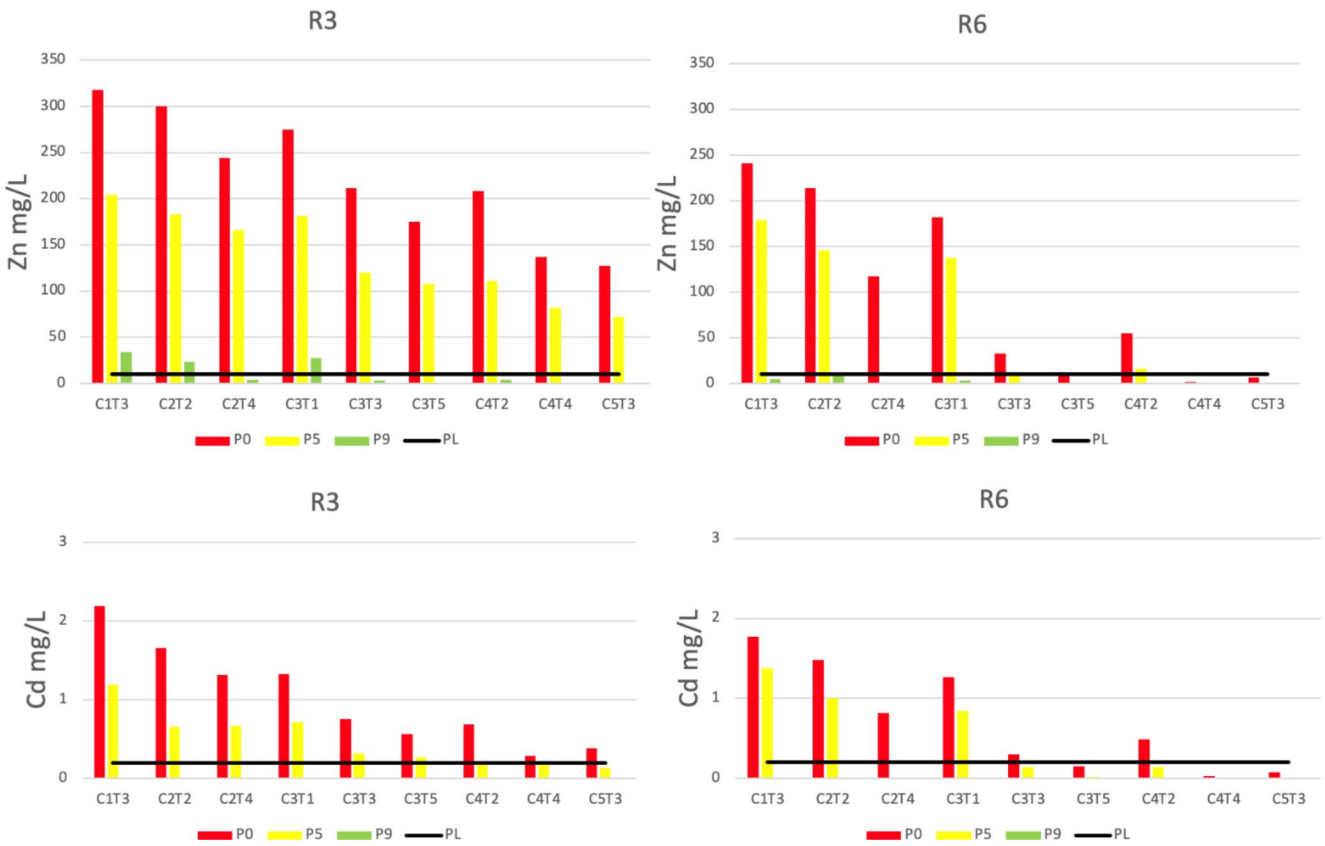

Fig. 3 Cd^{2+} and Zn^{2+} concentrations (mg/L) determined by ICP-OES in the ADM of fifty-four tests from the experiment designed by Minitab software

The results of the extrapolation using Minitab software for Zn^{2+} are presented in Fig. 1 as contour plots of R3 and R6 Mn waste/15 mL AMD-P9 ratios vs. contact times (hours) with the final concentrations of Zn^{2+} in the treated AMD. The efficiency of Mn wastes in removing Zn^{2+} is proportional to the solid/liquid ratio and contact time. Blue indicates solid/liquid (s/l) ratios and contact times that reduce the Zn^{2+} concentration below its MPL, changing to green when the concentration increases. Using R3, the MPL of Zn^{2+} is reached at 30 h with a ratio of 1.5 g waste/15 mL AMD and at a ratio of 0.5 g/15 mL with a time of ≈120 h (Fig. 1). Conversely, when using R6 waste, the Zn concentration dropped to between 5 and 7.5 mg/L within 1 h or less and with a ratio of 1.0/15 mL or slightly lower (Fig. 1). At a lower ratio (0.5 g/15 mL), the contact time increased to ≈45 h. The figure for Cd^{2+} is not presented but is analogues to the Zn^{2+}.

In conclusion, these results show that R6 has a much better capacity and is more efficient than R3, demonstrating the potential of Mn oxides as excellent sorbents, as reported in the literature. However, before applying these promising results in a pilot plant, they must be confirmed with specific experiments.

Zeta Potential (ZP)

The ZP of R3 at pH 8.4 was − 64.8 mV and remained practically constant up to pH 6 (-60.0 mV and − 55.8 mV). At pH 5.8, the ZP changed to -38.4 mV, and at pH 4.7, the ZP value became positive at + 5.6 mV. At pH 3.2, it increased to + 21.8 mV. At pH 4.9, the ZP attained the isoelectronic point (ZP0), as shown in Fig. 4. The ZP of R6 remained constant from pH 8.7 to pH 6 (-52.3 mV, -53.8 mV, -54.8 mV). At pH 4.9, it changed to -17.2 mV, and at pH 2.6, the ZP became positive at + 16.8 mV. The ZP0 was found at pH 3.0, as indicated in Fig. 4.

After adding R3 and R6 to the AMD, the ZP increased proportionally with concentration and contact time. Trial R3C3T1 exhibited the most minor ZP increases, while R6-C3T5 showed the greatest.

In the final experiment, the ZP changes were measured while various Zn^{2+} concentrations were added to non-treated AMD (NT-AMD), (Fig. 5). The ZP of R3 was − 38.9 mV when in contact with NT-AMD and increased proportionally with the addition of Zn^{2+}. At a Zn^{2+} concentration of 5,000 mg/L, the ZP reached its maximum value of + 24.7 mV (Fig. 5). Conversely, the R6 waste consistently displayed positive ZPs, even with the original AMD without Zn^{2+} addition. The ZP values ranged from + 9.8 when in

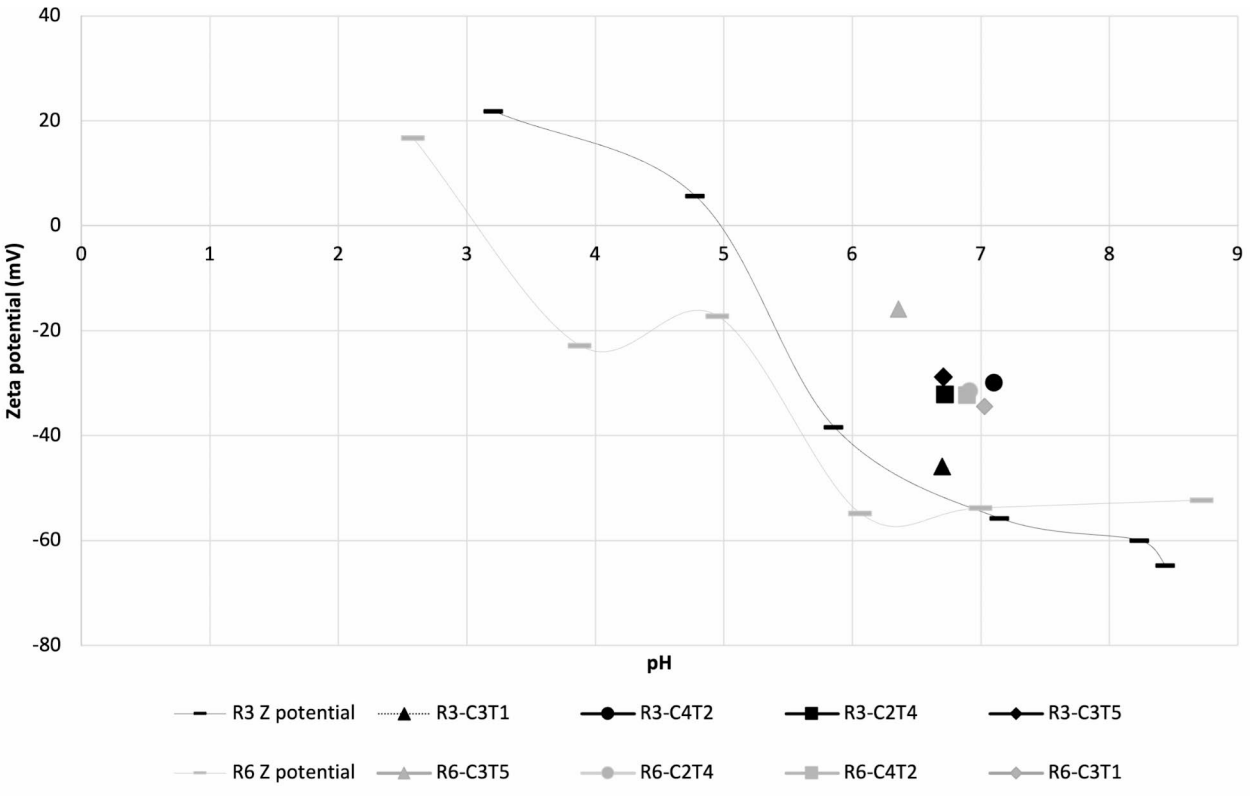

Fig. 4 Zeta potential of R3 and R6 wastes at different pH; t different concentrations (C2, C3 and C4) and contact times (T1, T2, T4 and T5). The ZP0 are indicated

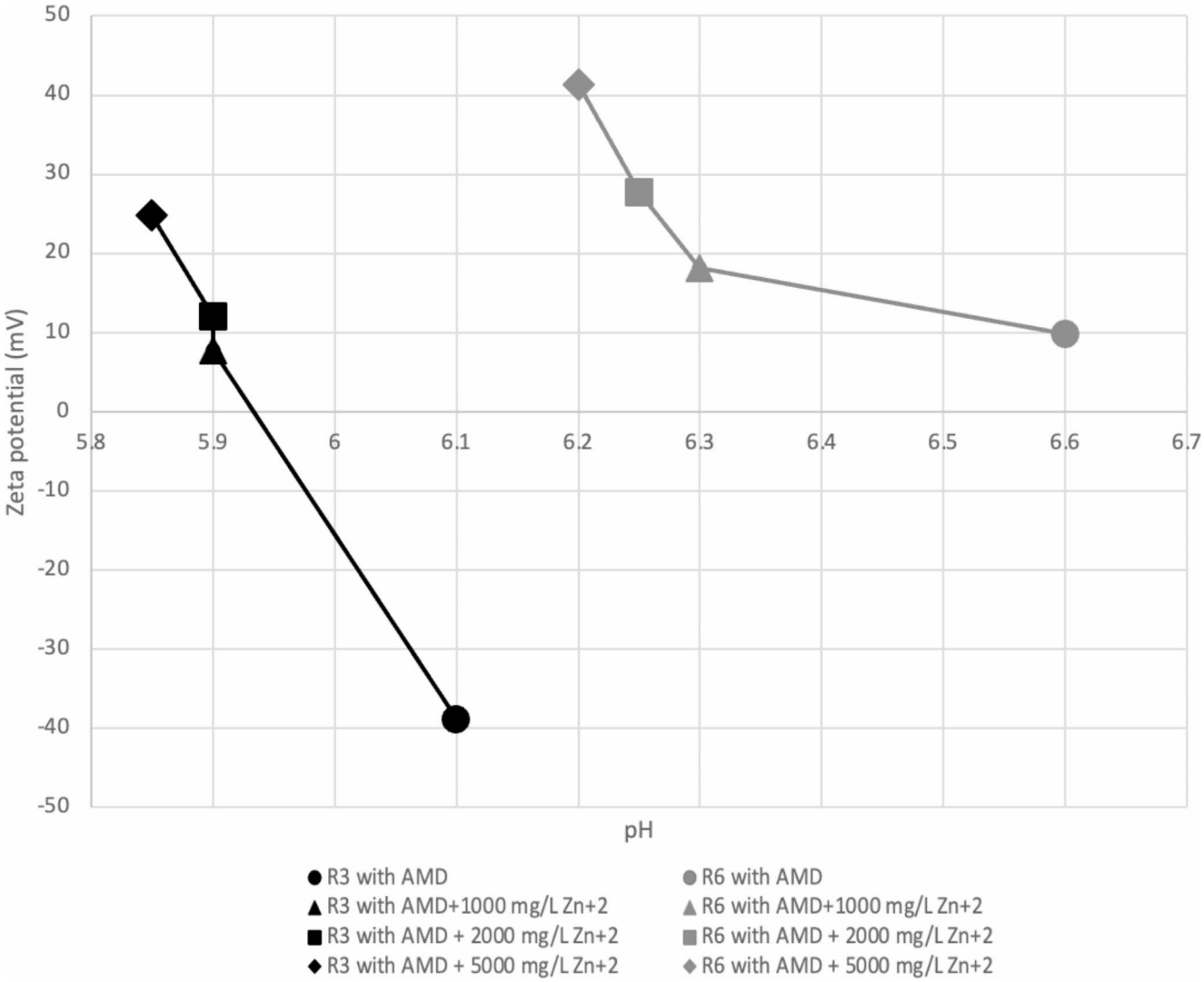

Fig. 5 Zeta potential of wastes + AMD, and with Zn^{2+} added at different concentrations

contact with NT-AMD to + 41.3 mV when exposed to AMD containing 5,000 mg/L Zn^{2+}.

Both wastes have a high sorption capacity, although the R6-waste provided a better outcome, which is consistent with its higher concentration of Mn oxides. The manganese carbonate in R6 increases the AMD's pH, favoring the negative charge of the oxide's surface and, consequently, enhances the adsorbing capacity. Similar results have been reported for organic and inorganic pollutant sorption using synthesized Mn_xO_y (Chowdhury et al. 2009; Della et al. 2013; Feng et al. 2007; Zhao et al. 2016). The surfaces of the finest particles in R3 and R6 are rich in Mn carbonates or oxides, creating a basic micro-environment with negative charges that favor adsorption and co-precipitation. Inner complexes may possibly be formed by exchanging Mn^{2+} from the carbonates with Zn^{2+} or Cd^{2+} from the solution, or they might be co-precipitated as hydroxy sulfates (Zhizhaev and Merkulova 2014) or hydroxy silicates (Kent and Kastner 1985). All these results with the Mn wastes highlight that sorption is the controlling process for cation removal and allows us to assume that these wastes can likely be used in other contaminant removal processes.

Sequential Extraction

A sequential extraction was conducted to assess the stability of the Cd, Mn, and Zn sorption bonds on the surfaces of the Mn wastes, as well as the stability of potential precipitates. The method followed Tessier's protocol (1979), excluding the organic phase due to the absence of organic compounds in the wastes. Supplemental Table S-9 displays the concentration distribution, with the highest concentration observed in the residual phase, which remained stable under environmental conditions. Solubilized concentrations

in other phases in which more labile ions are recovered, such as exchangeable carbonates and Fe-Mn oxides, were below the permissible levels set by Mexican regulations for river discharge, indicating effective cation retention. Table S-9 presents the findings from three trials. Similar trends were observed in the remaining trials, which demonstrated efficient Cd and Zn removal from the pretreated AMD (data not presented). Concentrations of Cd and Zn resolved from the extraction were also below their permissible levels.

Conclusions

Overall, our findings suggest that the Mn wastes can absorb cations from AMD without the alkaline pretreatment; however, larger quantities are necessary. In this scenario, the optimal strategy involves using a mixture of R3, enriched in carbonates, and R6, containing Mn-Fe oxides. R3 primarily acts as a neutralizing agent, while R6 is the sorbent material. Considering the high volumes of R3 and R6 wastes produced and stored at the Mn mine, the amount required for AMD treatment is readily available.

Incorporating R3 and R6 wastes into pretreated AMD at specific contact times and solid-to-liquid ratios effectively reduced Zn^{2+} and Cd^{2+} concentrations below their MPLs. Extended contact times or higher solid-to-liquid ratios further decreased final concentrations to levels below their LODs. While precipitation and sorption both contribute to contaminant removal by the Mn wastes, the results suggest that sorption plays a primary role.

Pretreatment with alkaline materials from the region enhances efficiency, reduces process costs by mitigating acidity, and precipitates several cations, thereby reducing the volume of Mn waste needed. Consequently, pretreating AMD enhances both the technical and economic viability of the treatment process.

This study, supported by existing literature, demonstrates the potential of Mn wastes to efficiently eliminate various pollutants from industrial drainage and water owing to their favorable adsorption characteristics. The results also indicate a commercial opportunity for selling the two wastes for other uses, facilitating their recycling. However, despite the favorable outcomes, additional experiments are necessary to evaluate the waste's recycling potential and optimize AMD treatment costs. A pilot test is essential to assess the feasibility of the proposed sorption process at an industrial scale and identify critical parameters.

The results obtained suggest that this process can be economically applied, although conditioned to the success of complementary experiments. Also, its implementation must involve the relevant stakeholders, mainly the community where the site is located. Also, when the process is in operation, long-term monitoring will be necessary to assess the system's behavior to ensure that the decrease in EPT concentrations continues to comply with the established limits and to assess the longevity of the treatment system. In the extreme case of the system's failure, other alternatives must be explored, including active treatment, though its viability depends on obtaining the necessary long-term funding from the government or private foundations.

Utilizing Mn wastes for AMD treatment simultaneously tackles two environmental concerns. First, it reduces the accumulation of solid wastes in open areas while treating the AMD, thereby mitigating ecological risks in both zones. Second, it exemplifies a circular economy solution, safeguarding the environment and contributing to waste valorization.

Supplementary Information The online version contains supplementary material available at https://doi.org/10.1007/s10230-024-01003-2.

Acknowledgements The authors are very grateful to Dr. Francisco Romero and Dr. Gerardo Martinez for their support in collecting the samples and giving important information, to Q.F.B. Reyna Roldan and M.Sc. Alfredo Jimenez for their help in the chemical analyses, and to Sonia Helen Ponce Wainer for her grammatical revisions.

Data availability The information is shown in Table 1.

References

Al-Degs Y, Khraisheh MAM, Tutunji MF (2001) Sorption of lead ions on diatomite and manganese oxides modified diatomite. Water Res 35(15):3724–3728. https://doi.org/10.1016/S0043-1354(01)00071-9

Balintova M, Petrilakova A (2011) Study of pH influence on selective precipitation of heavy metals from acid mine drainage. Chem Eng Trans 25:1–6. https://doi.org/10.3303/CET1125058

Berghorn GH, Hunzeker GR (2001) Passive treatment alternatives for remediating abandoned-mine drainage. Remediation J 11(3):111–127. https://doi.org/10.1002/rem.1007

Bower JA, Lister S, Hazebrouck G, Perdrial N (2017) Geospatial evaluation of lead bio-accessibility and distribution for site specific prediction of threshold limits. Environ Pollut 229:290–299. https://doi.org/10.1016/j.envpol.2017.05.064

Chowdhury AN, Azam MS, Aktaruzzaman M, Rahim A (2009) Oxidative and antibacterial activity of Mn_3O_4. J Hazard Mater 172(2–3):1229–1235. https://doi.org/10.1016/j.jhazmat.2009.07.129

Cravotta IIICA (2021) Interactive PHREEQ-N-AMDTreat water-quality modeling tools to evaluate performance and design of treatment systems for acid mine drainage. Appl Geochem 126:104845. https://doi.org/10.1016/j.apgeochem.2020.104845

Della Puppa L, Komárek M, Bordas F, Bollinger JC, Joussein E (2013) Adsorption of copper, cadmium, lead and zinc onto a synthetic manganese oxide. J Colloid Interface Sci 399:99–106. https://doi.org/10.1016/j.jcis.2013.02.029

Demirkiran N (2015) Copper adsorption by natural manganese dioxide. T Nonferr Met Soc China 25(2):647–653. https://doi.org/10.1016/S1003-6326(15)63648-2

Dyer A, Pillinger M, Newton J, Harjula R, Möller T, Amin S (2000) Sorption behavior of radionuclides on crystalline synthetic tunnel manganese oxides. Chem Mater 12(12):3798–3804. https://doi.org/10.1021/cm001142v

Environmental Protection Agency (2004) Method 9045D: Soil and waste pH. www.epa.gov/hw-sw846/sw-846-test-method-9045d-soil-and-waste-ph

Environmental Protection Agency (2007) Method 6200 (SW-846): Field portable x-ray fluorescence spectrometry for the determination of elemental concentrations in soil and sediment. https://semspub.epa.gov › work › 09 › 1160906.pdf

Environmental Protection Agency (1996) Method 3052: Microwave assisted acid digestion of siliceous and organically based matrices. www.epa.gov/sites/production/files/2015-12/documents/3052.pdf

Environmental Protection Agency (2007) Method 3015A: Microwave assisted acid digestion of aqueous samples and extracts. https://www.epa.gov/sites/default/files/2015-12/documents/3015a.pdf

Environmental Protection Agency (1982) Method 120.1: Conductance (Specific Conductance, umhos at 25°C) by Conductivity Meter. https://www.epa.gov/sites/default/files/2015-08/documents/method_120-1_1982.pdf

Environmental Protection Agency (2000) Method 6010 C (SW-846): Inductively coupled plasma - atomic emission spectrometry. www.epa.gov/sites/production/files/2015-12/documents/3052.pdf

Feng XH, Zhai LM, Tan WF, Liu F, He JZ (2007) Adsorption and redox reactions of heavy metals on synthesized mn oxide minerals. Environ Pollut 147(2):366–373. https://doi.org/10.1016/j.envpol.2006.05.028

Ford KL (2003) Passive Treatment Systems for Acid Mine Drainage. U.S. Bureau of Land Management. https://digitalcommons.unl.edu/usblmpub/19

Hengen TJ, Squillace MK, O'Sullivan AD, Stone JJ (2014) Life cycle assessment analysis of active and passive acid mine drainage treatment technologies. Resour Conserv Recycl 86:160–167. https://doi.org/10.1016/j.resconrec.2014.01.003

Hesse PR, Hesse PR (1971) A textbook of soil chemical analysis. Cambridge University Press. https://doi.org/10.1017/S0014479700005202

Islam MA, Morton DW, Johnson BB, Mainali B, Angove MJ (2018) Manganese oxides and their application to metal ion and contaminant removal from wastewater. J Water Process Eng 26:264–280. https://doi.org/10.1016/j.jwpe.2018.10.018

Kent DB, Kastner M (1985) Mg2 + removal in the system Mg2+—amorphous SiO2—H2O by adsorption and Mg-hydroxysilicate precipitation. GCA 49(5):1123–1136. https://doi.org/10.1016/0016-7037(85)90003-1

Kumpiene J (2010) In: Hooda PS (ed) Trace element immobilization in soil using amendments. Blackwell Publishing Ltd., pp 353–379. https://doi.org/10.1002/9781444319477

Martínez NM, Basallote MD, Meyer A, Cánovas CR, Macías F, Schneider P (2019) Life cycle assessment of a passive remediation system for acid mine drainage: towards more sustainable mining activity. J Clean Prod 211:1100–1111. https://doi.org/10.1016/j.jclepro.2018.11.224

McKenzie RM (1972) The sorption of some heavy metals by the lower oxides of manganese. Geoderma 8(1):29–35. https://doi.org/10.1016/0016-7061(72)90030-4

Meza-Figueroa D, Barboza-Flores M, Romero FM, Acosta-Elias M, Hernández-Mendiola E, Maldonado-Escalante F, Pedroza-Montero M (2020) Metal bioaccessibility, particle size distribution and polydispersity of playground dust in synthetic lysosomal fluids. Sci Total Environ 713:136481. https://doi.org/10.1016/j.scitotenv.2019.136481

Molina-Reyes MA, Piñon-Flores LF (2019) Utilización de un residuo proveniente de una planta nodulizadora de $MnCO_3$ para el manejo de drenaje ácido. Diss, Universidad Nacional Autónoma de México (in Spanish). https://hdl.handle.net/20.500.14330/TES01000790551

Park I, Tabelin CB, Jeon S, Li X, Seno K, Ito M, Hiroyoshi N (2019) A review of recent strategies for acid mine drainage prevention and mine tailings recycling. Chemosphere 219:588–606. https://doi.org/10.1016/j.chemosphere.2018.11.053

Pérez-Corrales D (2015) Evaluación de diferentes materiales geológicos para el tratamiento pasivo del drenaje ácido de minas, en Taxco-Guerrero. PhD Thesis, Programa Posgrado en Ciencias de la Tierra. Universidad Nacional Autónoma de México (in Spanish). https://hdl.handle.net/20.500.14330/TES01000723805

Ramos-Perez D, Alcántara-Hernández RJ, Romero FM, González-Chávez JL (2022) Changes in the prokaryotic diversity in response to hydrochemical variations during an acid mine drainage passive treatment. Sci Total Environ 842:156629. https://doi.org/10.1016/j.scitotenv.2022.156629

Romero FM, Núñez L, Gutiérrez ME, Armienta MA, Ceniceros-Gómez AE (2011) Evaluation of the potential of indigenous calcareous shale for neutralization and removal of arsenic and heavy metals from acid mine drainage in the Taxco mining area, Mexico. Arch Environ Contam Toxicol 60(2):191–203. https://doi.org/10.1007/s00244-010-9544-z

RoyChowdhury A, Sarkar D, Datta R (2015) Remediation of acid mine drainage-impacted water. Curr Pollut Rep 1:131–141. https://doi.org/10.1007/s40726-015-0011-3

Ryu JG, Kim Y (2022) Mineral transformation and dissolution of jarosite coprecipitated with hazardous oxyanions and their mobility changes. J Hazard Mater 427:128283. https://doi.org/10.1016/j.jhazmat.2022.128283

Taylor J, Pape S, Murphy N (2005) A summary of passive and active treatment technologies for acid and metalliferous drainage (AMD). Proc, 5th Australian Workshop on Acid Drainage Vol 29, pp 1–49

Tessier A, Campbell PGC, Bisson M (1979) Sequential extraction procedure for the speciation of particulate trace metals. Anal Chem 51(7):844–851

Trumm D (2010) Selection of active and passive treatment systems for AMD—flow charts for New Zealand conditions. New Z J Geol Geophys 53(2–3):195–210. https://doi.org/10.1080/00288306.2010.500715

Turner A, Lewis M (2018) Lead and other heavy metals in soils impacted by exterior legacy paint in residential areas of southwest England. Sci Total Environ 619–620:1206–1213. https://doi.org/10.1016/j.scitotenv.2017.11.041

Wang T, Liu Y, Deng Y, Cheng H, Fang X, Zhang L (2020) Heterogeneous formation of sulfur species on manganese oxides: effects of particle type and moisture condition. J Phys Chem A 124(36):7300–7312. https://doi.org/10.1021/acs.jpca.0c04483

Webster JG, Swedlund PJ, Webster KS (1998) Trace metal adsorption onto an acid mine drainage iron (III) oxy hydroxy sulfate. Environ Sci Technol 32(10):1361–1368. https://doi.org/10.1021/es9704390

Wick S, Peña J, Voegelin A (2019) Thallium sorption onto manganese oxides. Environ Sci Technol 53(22):13168–13178. https://doi.org/10.1021/acs.est.9b04454

Xiong Y, Tong Q, Shan W, Xing Z, Wang Y, Wen S, Lou Z (2017) Arsenic transformation and adsorption by iron hydroxide/manganese dioxide doped straw activated carbon. Appl Surf Sci 416:618–627. https://doi.org/10.1016/j.apsusc.2017.04.145

Yang Y, Li B, Li T, Liu P, Zhang B, Che L (2023) A review of treatment technologies for acid mine drainage and sustainability assessment. J Water Process Eng 55:104213. https://doi.org/10.1016/j.jwpe.2023.104213

Zhang YX, Jia Y (2018) Fluoride adsorption on manganese carbonate: ion-exchange based on the surface carbonate-like groups and hydroxyl groups. J Colloid Interface Sci 510:407–417. https://doi.org/10.1016/j.jcis.2017.09.090

Zhang C, Yu Z, Zeng G, Huang B, Dong H, Huang J, Zhang Q (2016) Phase transformation of crystalline iron oxides and their adsorption abilities for pb and cd. Chem Eng J 284:247–259. https://doi.org/10.1016/j.cej.2015.08.096

Zhang H, Xu F, Xue J, Chen S, Wang J, Yang Y (2020) Enhanced removal of heavy metal ions from aqueous solution using manganese dioxide-loaded biochar: behavior and mechanism. Sci Rep 10(1):6067. https://doi.org/10.1038/s41598-020-63000-z

Zhao M, Xu Y, Zhang C, Rong H, Zeng G (2016) New trends in removing heavy metals from wastewater. Appl Microbiol Biotechnol 100(15):6509–6518. https://doi.org/10.1007/s00253-016-7646-x

Zhizhaev AM, Merkulova EN (2014) Interaction of copper (II) and zinc (II) in coprecipitation from sulfate solutions with natural calcium carbonate. Russ J Appl Chem 87:16–22. https://doi.org/10.1134/S1070427214010029

Authors and Affiliations

Luis F. Piñon-Flores[1] · Margarita E. Gutiérrez-Ruiz[1] · José L. González-Chávez[1] · Daniel E. Amaro-Ramírez[1] · Arturo Aguirre-Gómez[2] · Marco A. Molina-Reyes[1]

✉ Margarita E. Gutiérrez-Ruiz
ginny@unam.mx

[1] Facultad de Química, Universidad Nacional Autónoma de México, Ciudad de, Mexico

[2] Facultad de Estudios Superiores Cuautitlán Campo 4, , Universidad Nacional Autónoma de México, Cuautitlán Izcalli, Estado de, Mexico